OXFORD

ORIGINAL ARTICLE

Timing of Cortico-Muscle Transmission During Active Movement

Gustaf M. Van Acker III[1], Carl W. Luchies[2,3], and Paul D. Cheney[1]

[1]Department of Molecular and Integrative Physiology, University of Kansas Medical Center, Kansas City, KS 66160, USA, [2]Bioengineering Graduate Program and [3]Department of Mechanical Engineering, University of Kansas, Lawrence, KS 66045, USA

Address correspondence to Dr Paul D. Cheney, Department of Molecular and Integrative Physiology, University of Kansas Medical Center, 3901 Rainbow Blvd, Mail Stop 3043, Kansas City, KS 66160-7336, USA. Email: pcheney@kumc.edu

Abstract

Numerous studies have reported large disparities between short cortico-muscle conduction latencies and long recorded delays between cortical firing and evoked muscle activity. Using methods such as spike- and stimulus-triggered averaging of electromyographic (EMG) activity, previous studies have shown that the time delay between corticomotoneuronal (CM) cell firing and onset of facilitation of forelimb muscle activity ranges from 6.7 to 9.8 ms, depending on the muscle group tested. In contrast, numerous studies have reported delays of 60–122 ms between cortical cell firing onset and either EMG or movement onset during motor tasks. To further investigate this disparity, we simulated rapid active movement by applying frequency-modulated stimulus trains to M1 cortical sites in a rhesus macaque performing a movement task. This yielded corresponding EMG modulations, the latency of which could be measured relative to the stimulus modulations. The overall mean delay from stimulus frequency modulation to EMG modulation was 11.5 ± 5.6 ms, matching closely the conduction time through the cortico-muscle pathway (12.6 ± 2.0 ms) derived from poststimulus facilitation peaks computed at the same sites. We conclude that, during active movement, the delay between modulated M1 cortical output and its impact on muscle activity approaches the physical cortico-muscle conduction time.

Key words: cortico-muscle delay, EMG, forelimb, motor control, primary motor cortex

Introduction

The synaptic connectivity between the primary motor cortex (M1) and motoneurons has been studied extensively (Porter and Lemon 1993; Morrow and Miller 2003; Rathelot and Strick 2006; Townsend et al. 2006; Schieber and Rivlis 2007; Rathelot and Strick 2009). Using methods such as spike-triggered averaging (SpTA) and stimulus-triggered averaging (StTA) of electromyography (EMG) activity, previous studies have shown that the mean time delay between corticomotoneuronal (CM) cell firing and the onset of facilitation of distal forelimb muscle activity ranges from 6.7 to 9.8 ms, depending on the forearm muscle group tested (Cheney and Fetz 1980; Lemon et al. 1986; McKiernan et al. 1998; Park et al. 2004). These delays are consistent with the estimated conduction time from cerebral cortex to forelimb muscle

(Humphrey and Corrie 1978; Cheney and Fetz 1985; Baker and Lemon 1998).

In contrast, numerous studies have reported mean delays of 60–122 ms between the onset of cortical cell firing and the onset of EMG activity or natural movement (Evarts 1972; Porter and Lewis 1975; Thach 1975; Cheney and Fetz 1980; Lamarre et al. 1981; Wannier et al. 1991; Porter and Lemon 1993). Of course, it should be noted that excitation–contraction coupling would be expected to add as much as 50 ms to onset time in experiments that have measured cortical cell onset relative to the onset of movement or force (Begovic et al. 2014). In other studies, delays of 40–50 ms have been used to produce optimal correlations between EMG activity and M1 neurons (Morrow and Miller 2003; Townsend et al. 2006). These delays, coupled with the time

delay of 60–122 ms observed between the onset of cortical activity and EMG activity, have been used as a rationale for phase shifting the timing between cortical cell activity and muscle activity in studies of cortical encoding of EMG activity (Morrow and Miller 2003; Townsend et al. 2006; Schieber and Rivlis 2007).

Various hypotheses have been suggested to account for the timing discrepancies observed in these studies compared with the minimum conduction time over the corticospinal pathway measured with SpTA and StTA. One hypothesis is that plateau potentials, caused by persistent inward currents in the dendrites of motoneurons, may delay the transmission of incoming signals (Morrow and Miller 2003). These plateau potentials may utilize slow L-type Ca^{2+} channels and act as low-pass filters that amplify and substantially delay the incoming signals.

Another hypothesis is that motoneurons may require integration of signals from both direct corticospinal pathways and indirect, multisynaptic pathways (Schieber and Rivlis 2007). Requiring input from multisynaptic pathways could increase the delay from cortical activity to EMG activity, although it would require a very indirect route to account for the large phase shift discrepancy between the minimum conduction time and the cortical cell to muscle onset time measured during active movement.

Yet, another possibility is that the disparity could be due to the time required for motoneurons to achieve firing threshold from a quiescent state, which requires summation of converging excitatory postsynaptic potentials (EPSPs) from corticospinal and other inputs as well as temporal summation of EPSPs from individual inputs (Porter and Lewis 1975). The need for this type of synaptic summation could significantly delay the initiation of movement; however, contrary to the first 2 hypotheses, time delays due to this mechanism should be reduced once motoneurons are actively firing.

While each of these hypotheses is plausible, the actual cause for the timing discrepancy remains unclear. In the current study, we investigated the delay between cortical activity and EMG activity during active movement, while the motoneurons were at or above firing threshold. We generated time-varying modulations of corticospinal output to motoneurons by applying frequency-modulated stimulus trains to individual M1 cortical sites on a background of active movement-related EMG activity. This procedure yielded corresponding modulations of EMG activity whose phase shift could be measured relative to modulations in the applied stimulus train. The phase shift results obtained could then be used to examine whether or not the large delays seen in other studies might be attributable largely to the time required to bring motoneurons to firing threshold during initiation of movement.

The overall mean delay from the peak in stimulus frequency modulation to the peak in EMG modulation was 11.5 ± 5.6 ms, matching closely the conduction time through the cortex-to-muscle pathway of 12.6 ± 2.0 ms derived from the peak of poststimulus facilitation computed at the same sites. While the 3 hypotheses mentioned above may not be mutually exclusive, with each contributing to delays between cortical firing and muscle activation, the results in this study support the hypothesis that the longer time delays reported for the timing between cortical cell activation and muscle activation are due largely to the time required to bring motoneurons to firing threshold from a hyperpolarized state.

Materials and Methods

Behavioral Task

We trained a male rhesus macaque (*Macaca mulatta*) to perform a ramp-and-hold concentric wrist task described in detail previously (Mewes and Cheney 1991). Briefly, the monkey was seated in a custom primate chair within a sound-attenuating chamber with his arms comfortably restrained bilaterally. His right elbow was positioned at a 90° angle, and his right hand was positioned with palm vertical and fingers extended in a manipulandum that allowed horizontal concentric rotation about the wrist while restricting abduction and adduction, allowing for isolation of flexor and extensor muscle activity. To receive an applesauce reward, the monkey was required to produce alternating ramp-and-hold wrist movements to target positions of 40° ± 10 in flexion and 30° ± 15 in extension for a period of 1 s, with 0° being alignment of the wrist with the forearm. Wrist movements were made against moderate spring-like loads generated by a torque motor connected to the axis of the manipulandum, with the resistance calculated to be 8.33×10^{-4} Nm per degree of rotation. Performance was guided by audio and visual cues.

Surgical Procedures

Following training, an MRI-compatible stainless steel chamber, allowing a 30-mm diameter dural exposure and exploration of the underlying cortical area, was implanted stereotaxically over the primary motor cortex of the left hemisphere using procedures described in detail previously (Park et al. 2000). Briefly, the chamber was anchored to the skull using titanium screws and dental acrylic, and was centered over the hand area of M1 in the left hemisphere. In addition, threaded titanium nuts were attached over the occipital aspect of the skull using titanium screws and dental acrylic. These nuts provided a point of attachment for a flexible head-restraint system during recording (McKiernan et al. 1998, 2000).

Muscles of the right forearm, 5 flexors and 5 extensors, were each implanted with 2 multistranded stainless steel wires (Cooner Wire, AS632) using a transcutaneous technique described in detail previously (McKiernan et al. 2000). Briefly, all wires were stripped of approximately 2–3 mm of insulation and inserted transcutaneously into the target muscles a distance of approximately 2–3 cm, with about 5 mm separation of the 2 wires in each muscle. The wires terminated in connector modules (ITT Cannon, New Britain, CT, USA) placed on the forearm. We tested the placement accuracy of each electrode pair by observing appropriate muscle twitches resulting from short stimulus trains. After confirming placement accuracy of all electrodes, medical adhesive tape was used to secure wires and the connectors to the forearm for the duration of the implant. The monkey wore a full-sleeved jacket (Lomir Biomedical, model PJ05) while in his home cage, with the right arm of the jacket reinforced with stainless steel mesh (Saf-T-Gard, Type 4.2 stainless steel mesh) to protect the implant.

We recorded multiunit EMG activity from 5 extensor muscles: Extensor carpi radialis (ECR), extensor digitorum communis (EDC), extensor digitorum 4,5 (ED4,5), extensor carpi ulnaris (ECU), and extensor digitorum 2,3 (ED2,3); and 5 flexor muscles: Flexor carpi radialis (FCR), flexor digitorum superficialis (FDS), palmaris longus (PL), flexor carpi ulnaris (FCU), and flexor digitorum profundus (FDP).

Prior to each implant surgery, the monkey was administered ketamine (10 mg/kg, IM), atropine (0.04 mg/kg IM), medetomidine (0.05 mg/kg IM), and subsequently isoflurane gas for the duration of the surgery. The monkey received prophylactic antibiotic (penicillin, 6000 U/kg, SC) 10 h presurgery, 1 h postsurgery, and 3 days subsequent to the surgery. Following the surgery, the monkey was given analgesics (buprenorphine, 0.01 mg/kg IM

and carprofen, 5 mg/kg SC). All surgeries were performed in a facility accredited by the Association for Assessment and Accreditation of Laboratory Animal Care using full sterile procedures. All procedures conformed to the Guide for the Care and Use of Laboratory Animals, published by the United States Department of Health and Human Services and the National Institutes of Health.

Data Recording

We stimulated multiple locations in the arm representation of primary motor cortex of the left hemisphere (Fig. 1) using glass- and mylar-insulated platinum–iridium electrodes with typical impedances of 0.7–1.5 MΩ (FHC, Inc., Bowdoin, ME, USA). We positioned the recording electrode using an X–Y positioner secured to the chamber for the duration of each recording session, and advanced the electrode into the brain using a manual hydraulic microdrive (FHC Corp.) until the electrode tip was located in cortical lamina V, or approximately 1.5 mm below the surface of the brain. Location of layer V was determined by depth, the appearance of large spikes, and finally by appropriate effects in StTA at 15 μA and 15 Hz.

Stimulus-Triggered Averages

StTAs were gathered for all implanted muscles from stimuli applied throughout all phases of the concentric wrist task. StTAs were used to help confirm positioning of the electrode in lamina
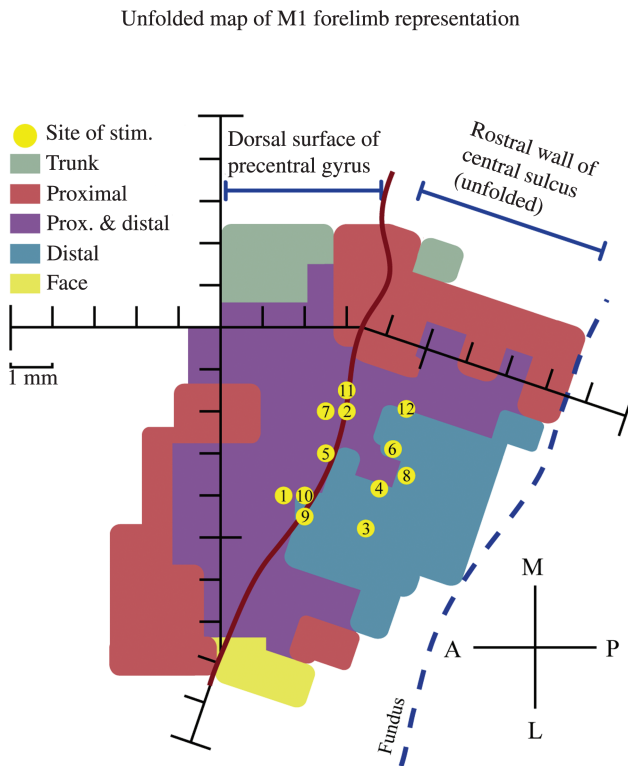

Figure 1. Unfolded map of the monkey's M1 forelimb representation in the left hemisphere with a view of the dorsal surface of the precentral gyrus and the rostral wall of the central sulcus. Anterior, posterior, medial, and lateral are indicated by the compass rose. Sites of frequency-modulated sinusoidal stimulation are indicated by the yellow dots, and are numbered in chronological order of stimulation. The color-coded muscle representation map was obtained from a previous StTA mapping study in this monkey (Griffin et al. 2014). Each hash mark represents a distance of 1 mm.
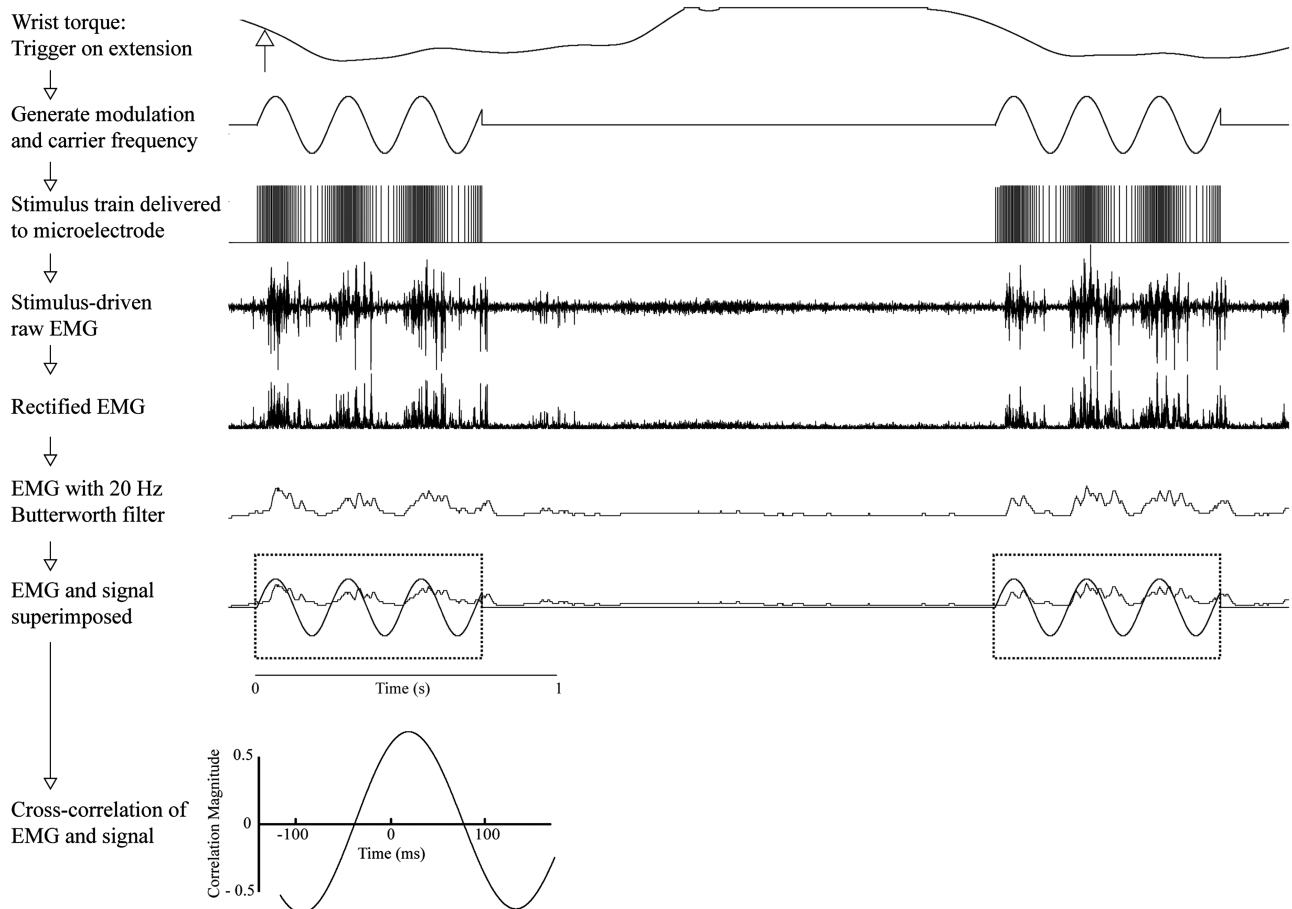
V, to confirm electrode location stability for the duration of each recording session, and to determine minimum conduction time through the cortico-muscle pathway. EMG activity was typically filtered from 30 Hz to 1 kHz, digitized at 4 kHz, and full-wave rectified. Individual stimuli for the StTAs were symmetrical biphasic pulses: An initial negative pulse 0.2 ms in duration followed directly by a positive pulse of 0.2 ms in duration. StTAs were based on a minimum of 500 trigger events. Averages were compiled using a 60-ms epoch, of which 20 ms prior to the trigger was considered baseline. StTAs were identified as having significant poststimulus effects if the peak or trough of the effect exceeded ±2SD of the baseline for a period of ≥0.75 ms or more as described previously (Park et al. 2004). Strong poststimulus effects suggested that the electrode tip was in layer V.

Frequency-Modulated Stimulation Protocol

Once we confirmed that the electrode tip was situated in or near layer V, we recorded the baseline EMG activity of all muscles during the concentric wrist task for both extension and flexion phases. We then initiated a stimulation protocol using specific combinations of the following parameters: Current intensity (10, 15, and 30 μA), stimulus train carrier frequency (100, 150, 200, and 250 Hz), modulation frequency (4, 12, and 28 Hz), and extension- or flexion-triggered stimulation. We used the same stimulation protocol at each cortical site whenever possible. For each stimulus parameter, a minimum of 50 trials were collected to compute an average EMG response to modulated stimulation. The stimulus trains were separated by a sufficient rest period to ensure that trains applied at the beginning and end of a parameter set evoked similar EMG responses.

To generate the frequency-modulated sinusoidal stimulus trains, a waveform generator producing a sinusoidal output was triggered by either wrist flexion or extension (Fig. 2). This signal modulated the simultaneously triggered stimulus train carrier frequency created by a second waveform generator. The rising phase of this synthesized frequency-modulated signal triggered a Grass S-88 stimulator, which, in turn, delivered biphasic electrical pulses to the cortex via the microelectrode. The peak of the sinusoidal signal used to modulate the stimulus train carrier frequency co-varied directly in time with the peak stimulus frequency, such that the shortest interstimulus interval in the frequency-modulated stimulus train coincided precisely with the peak of the sinusoidal signal. Therefore, we used the sinusoidal modulating signal for analog cross-correlation analysis, an example of which is shown as the final step in Figure 2.

Measurement of EMG Cross-Talk

We evaluated cross-talk between EMG electrodes by constructing EMG-triggered averages. This procedure used the motor unit potentials from one muscle as triggers for compiling averages of rectified EMG activity of all other muscles. The criterion established by Buys et al. (1986) was used to eliminate effects that might have been affected by cross-talk. To be accepted as a valid poststimulus effect, the ratio of poststimulus facilitation between test and trigger muscles had to exceed the ratio of their cross-talk peaks by a factor of 2 or more. Based on this criterion, no effect had to be eliminated.

Measurement of Delay

Once we acquired the EMG responses to sinusoidal stimulation, we applied an offline interpolation method to remove any

Figure 2. Methodology for stimulation, recording, and cross-correlation. Stimulation was applied either on wrist flexion or extension, applying a combination of modulation frequency and carrier frequency. Stimulation at this modulated frequency was delivered to the stimulating electrode at a set stimulus intensity, and the output electromyography (EMG) activity was recorded. This stimulus-driven EMG activity was then rectified and smoothed using a 20-Hz Butterworth filter. This smoothed and rectified EMG was then cross-correlated with the signal used to drive frequency modulation to determine the overall phase shift offset between the modulated stimulus delivered to the cortex and the resulting modulated EMG activity. Only sections of data in which stimulation was delivered were used for analysis (dotted boxes). Data in this example used a modulation frequency of 4 Hz, a carrier frequency of 150 Hz, and stimulation intensity of 30 µA; EMG was recorded from extensor carpi radialis (ECR) and triggered on wrist extension.

stimulus artifact present in the raw EMG (Windows Neural Averager, L. Shupe, University of Washington, Seattle, WA, USA).

We determined cortico-muscle transmission time by cross-correlating EMG activity with the sine wave used to produce stimulus train modulation. Because the process of preparing records for cross-correlation analysis, which involved eliminating periods with no stimulation and re-linking the records, was very time-consuming, we elected to quantify and perform analyses on the first 10 trials of stimulation. We noted that EMG responses generally did not change substantially in response to stimulation after 10 trials and confirmed this by computing cross-correlation analysis on all 50 trials for a subset of the data. We rectified the raw EMG and smoothed it using a second-order Butterworth low-pass filter, and applied the same filter to the modulating sine wave signal to control for possible phase shift associated with filtering. Cross-correlation significance level was determined by breaking the EMG signal into 10 parts, reassembling the parts randomly and then recomputing the correlation. This was repeated for 9 datasets. The overall correlation coefficient after randomizing the EMG signal was 0.1466, which is similar to significance estimates others have used (±0.15) for this type of data (Houk et al. 1987; Miller

et al. 1993). Accordingly, correlation coefficients of ±0.15 or greater were considered significant and used in subsequent analyses.

The onset of EMG activity relative to the onset of frequency-modulated stimulation was measured as the point at which the envelope of the EMG record surpassed the equivalent of ±2SD above or below the mean of the baseline EMG activity. We used the 125-ms epoch preceding stimulus onset for the baseline.

Results

Stimulus-Triggered Averages

StTAs were acquired at each cortical site at which frequency-modulated stimulation was applied, using the same current intensities used for modulated stimulation. Acquiring StTAs allowed us to determine the optimal locations to apply the frequency-modulated stimulus protocol. It also provided a measure of the minimum conduction time for cortico-muscle connections at a particular cortical site. The poststimulus facilitation (PStF) onset and peak latencies measured in this study (Table 1) are comparable with poststimulus facilitation effects seen in previous studies of the forelimb (Park et al. 2004).

Table 1 Mean latencies and magnitudes of poststimulus effects obtained from StTAs

	n	Onset (ms)	Peak (ms)	Magnitude (%)
PStF	253	9.6 ± 2.1	12.6 ± 2.0	72.5 ± 92.6
PStS	38	14.2 ± 2.8	17.7 ± 5.0	−21.8 ± 7.0

Note: Values are means ± SD. Stimulus intensities used to acquire StTAs were 10, 15, and 30 μA. Magnitude was measured as the peak increase above baseline for poststimulus facilitation (PStF) or decrease below baseline for poststimulus suppression (PStS) expressed as a percent of baseline.
n: number of effects measured.

Table 2 Comparison of effects from sinusoidal stimulation and stimulus-triggered averaging

Poststimulus effect	Sinusoidal stimulation effect			
	pE n	pI n	tEI n	Total n
PStF	488	79	332	899
PStS	21	34	20	75
PStF/PStS	64	17	51	132
Weak or no PStE	129	157	91	377
Total	702	287	494	1493

Note: Values are the total number of sinusoidal modulation effects across all stimulation sites corresponding to different types of poststimulus effects obtained from the same sites. Stimulus intensities used were 10, 15, and 30 μA. EMG modulation effects were considered significant and included if the envelope of the EMG record surpassed ±2SD above or below the mean of the baseline EMG activity.
pE: predominantly excitatory; pI: predominantly inhibitory; tEI: initially excitatory transitioning to inhibitory; n: number of measurements.

Sites that yielded strong PStF in StTAs were more likely to yield predominantly excitatory (pE) rather than inhibitory modulation when frequency-modulated stimulation was applied, whereas sites that yielded poststimulus suppression (PStS) were more likely to yield predominantly inhibitory (pI) modulation (Table 2). For example, the StTAs in Figure 3C show PStF in ED4,5 and, at a longer latency, weak PStS in FDP. Applying frequency-modulated stimulation produced pE modulation in ED4,5, and pI modulation in FDP (Fig. 3G). When FDP was silent (Fig. 3D), applying stimulation produced little or no appreciable modulation. However, when FDP was active (Fig. 3E), stimulation produced inhibition associated with peaks in the frequency of stimulation. The sign of the effect from frequency-modulated stimulation can be most readily appreciated by looking at the response to the initial cycle of the frequency-modulated stimulus train (Fig. 3G). Note that the response is clearly excitatory for ED4,5 (1) and inhibitory for FDP (2). Also of interest is the fact that the excitatory modulation of ED4,5 strengthens throughout the hold phase of the response, whereas the inhibitory modulation in FDP is diminished after the first 2 cycles.

Time Delays Derived from Analog Cross-Correlations

Cortical sites that yielded strong poststimulus effects in StTA records yielded robust EMG modulation in response to frequency-modulated stimulus trains applied at the same site, although sites that showed no poststimulus effects in StTA records also showed prominent EMG modulation with sinusoidal stimulation. Cortical sites yielding poststimulus facilitation in StTA most

commonly, but not always, produced EMG modulation that was purely excitatory (Table 2). The mean phase delay in cross-correlations computed at sites that produced no poststimulus effect (PStE) (12.3 ± 5.8, n = 129) was not statistically different from the phase delay for sites that produced PStF (11.4 ± 5.7, n = 488; P = 0.12). However, the cross-correlation magnitude for sites with PStF (0.36) was significantly greater than that for sites with no PStE (0.24, P < 0.001).

At all carrier frequencies, 3 fundamental modulation patterns in the EMG records were observed in response to stimulation: pE, pI, and initially excitatory transitioning to inhibitory (tEI). Predominantly excitatory responses yielded peaks in EMG activity that were directly related to corresponding peaks in stimulus frequency, that is, as stimulus frequency increased, EMG activity increased (Figs 3Gi and 4A). pI responses were those that yielded the inverse of this pattern, that is, as stimulus frequency increased, EMG activity decreased (Figs 3Gii and 4B). Responses categorized as tEI were those that shifted from excitatory to inhibitory over the course of the 750-ms trial (Fig. 4C). In rare cases (0.5% of total responses), the EMG response to frequency-modulated stimulation was inhibitory and then became excitatory with cycles later in the train.

Using cross-correlation analysis, we compared the time delay of peaks in EMG activity relative with corresponding peaks in stimulus frequency. Given that most pI and tEI effects did not modulate as clearly with sinusoidal stimulation as did pE effects, cross-correlation results for pI and tEI effects were more difficult to interpret. Therefore, only records with pE responses were included in our cross-correlation analysis.

Average time delays between the frequency-modulated stimulus train and EMG activity derived from analog cross-correlation analysis are given in Table 3. The results are categorized by modulating frequency and carrier frequency. As there was no statistical difference in the time delays observed for different forearm muscles (one-way ANOVA on ranks, P = 0.485), the latencies for all muscles were combined in the analysis. Higher carrier frequencies yielded fewer pE responses and correspondingly more pI and tEI responses, as evident from the number of records for each parameter. In addition, higher modulation rates and higher carrier frequencies yielded lower cross-correlation magnitudes. Higher frequencies would be expected to produce greater physiological spread, activating cells via trans-synaptic cortico-cortical mechanisms likely spreading beyond the sphere of direct activation (Jankowska et al. 1975). Higher frequencies would therefore have a greater probability of recruiting both excitatory and inhibitory circuits producing interference that would reduce the fidelity with which the cortico-motor system could follow such frequencies. EPSP properties and temporal summation also put a limit on the maximum following frequency of the EMG signal. Interestingly, the 12-Hz carrier frequency yielded a significantly smaller phase shift than 4 and 28 Hz (P < 0.001), but the reason for this difference is unclear.

Increasing stimulus intensity resulted in a significant decrease in time delay of EMG modulation with respect to the modulated stimulus train (one-way ANOVA on ranks, P = < 0.001). pE responses for all frequency parameters with a stimulus intensity of 10 μA had a mean phase shift (EMG peak followed stimulus frequency peak) of 12.8 ± 4.3 ms (n = 184). Responses at 15 μA had a mean phase shift of 11.9 ± 5.6 ms (n = 273), and responses at 30 μA had a mean phase shift of 9.9 ± 6.1 ms (n = 245). A possible explanation for this shift toward shorter delays is that higher intensities produce activation of greater numbers of corticospinal cells due to physical spread of stimulus current (Tehovnik 1996), and subsequently more rapid activation of motor units. PStF
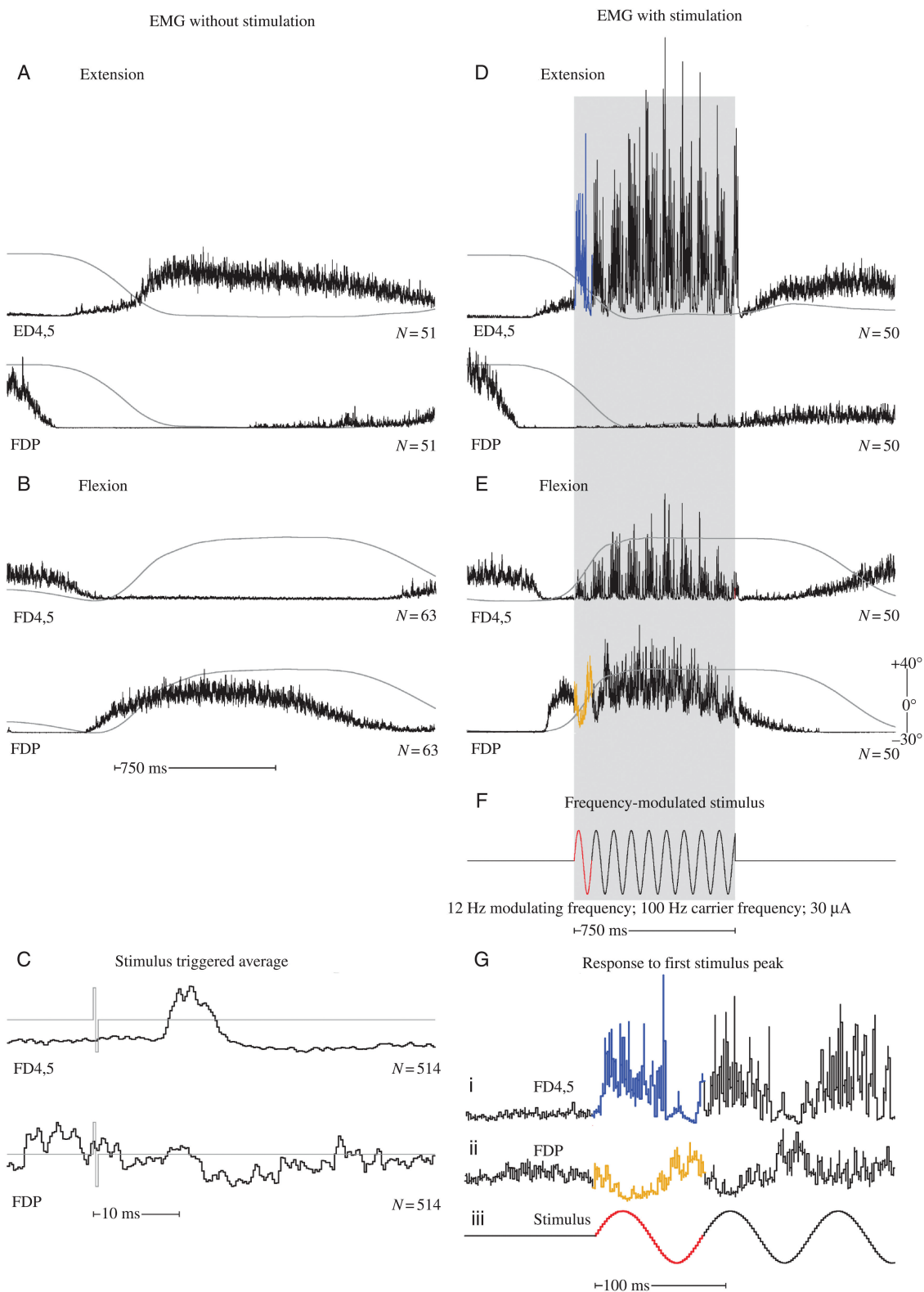
Figure 3. Baseline muscle activity and frequency-modulated activation of the same muscles. All records included in this figure were obtained from cortical site 5 (Fig. 1). (*A* and *B*) ED 4,5 and FDP EMG activity associated with wrist extension and flexion, respectively, in the absence of stimulation. (*C*) Stimulus-triggered averages for ED 4,5 and FDP acquired at 30 μA. The stimulus is shown as a light gray line superimposed on the EMG records. (*D* and *E*) Wrist extension and flexion, respectively, in response to frequency-modulated stimulation. The period of stimulation is represented by gray shading. (*F*) Frequency-modulated stimulation beginning midway through the dynamic phase of movement. (*G*) Response of ED4,5 during extension (i) and FDP during flexion (ii) in response to the first cycle of modulated stimulation (iii). Records are expansions of those in *D*, *E*, and *F* indicated by the corresponding colors. The number under each set of records is the number of events averaged. EMG activity has been uniformly scaled for each muscle. For muscle abbreviations, see Materials and Methods. Wrist position record (gray line) is superimposed on each EMG record, and ranges from 40° ± 10 in flexion to 30° ± 15 in extension. Upward deflection of the position record is flexion.
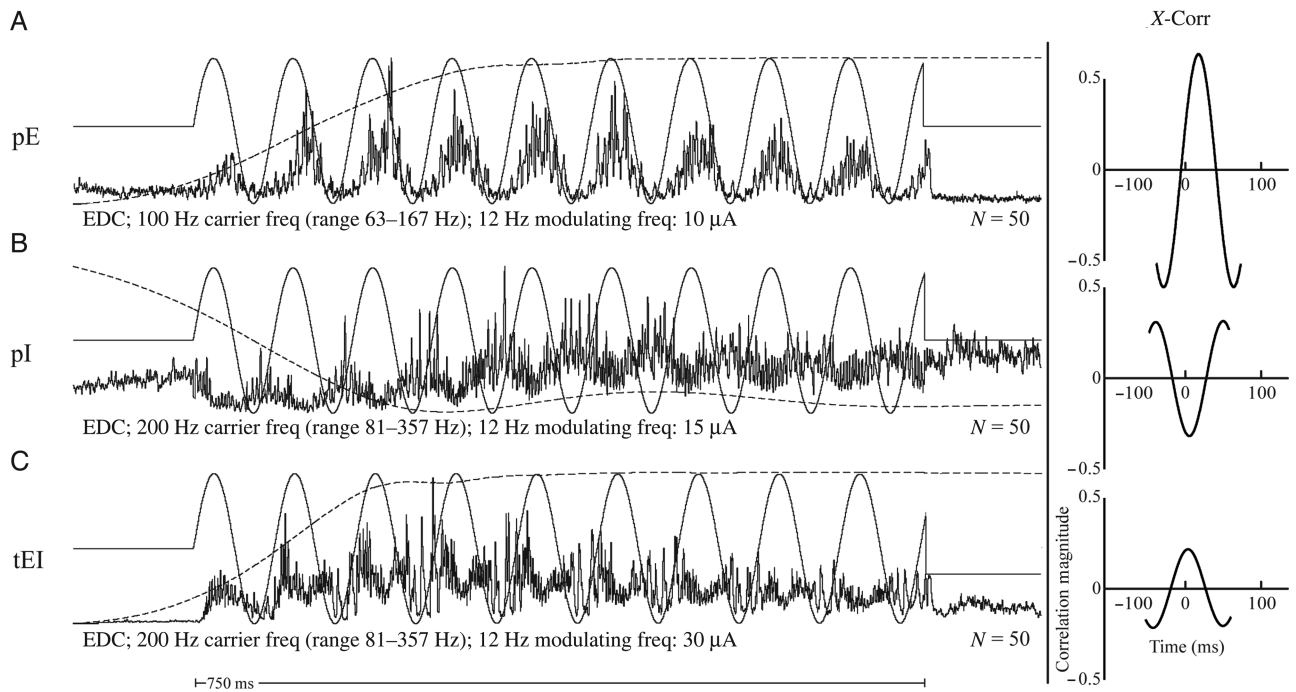
Figure 4. (A) pE response. EMG activity increases in response to increasing stimulus frequency. (B) pI response. EMG activity decreases in response to increasing stimulus frequency. (C) tEI, or excitation transitioning to inhibition. EMG activity initially responds with an increase in activity in response to increasing stimulus frequency, but gradually transitions to inhibition as the stimulus train continues. Cross-correlations are included on the right for each example. Vertical scale bar is the magnitude of correlation. For muscle abbreviations, see Materials and Methods. Wrist position record (dashed line) is superimposed on each EMG record, and ranges from 40° ± 10 in flexion (upward deflection) to 30° ± 15 in extension (downward deflection). The 12-Hz signal used to modulate the stimulus train is superimposed on the EMG records (solid sinusoidal line).

Table 3 Phase shift and magnitudes from analog cross-correlation analysis

Modulation frequency (Hz)	Carrier frequency (Hz)	Frequency range (Hz)	Phase shift (ms)	Magnitude (−1 to +1)	n
4	150	63–263	16.2 ± 7.8	0.46 ± 0.13	109
12	100	63–167	8.2 ± 4.5	0.38 ± 0.14	297
12	200	81–357	8.6 ± 5.5	0.28 ± 0.10	23
28	150	108–230	12.2 ± 2.3	0.24 ± 0.07	192
28	250	104–434	15.9 ± 1.9	0.19 ± 0.03	81
All	All	All	11.5 ± 5.6	0.33 ± 0.14	702

Note: Data based on the pE column of Table II. Values are means ± SD. Data are based on predominantly excitatory (pE) EMG modulation. Stimulus intensities used were 10, 15, and 30 µA. In all cases, EMG peak followed the stimulus frequency peak.
n: number of cortical site–muscle pairs measured; Magnitude %: peak percent increase (PPI) above baseline.

peak latencies for 10, 15, and 30 µA were 12.9 ± 2.5, 12.8 ± 1.7, and 12.2 ± 1.7 ms, respectively.

The overall mean time delay of pE EMG modulation including all parameters in this study was 11.5 ± 5.6 ms ($n = 702$). This delay approaches the minimum conduction time through the pathway from cortex to forearm muscles.

EMG Onset Measurements

We measured the onset of EMG activity following the onset of frequency-modulated stimulation for all pE M1 cortical sites in the study. The mean latency for all stimulus parameters was 10.7 ± 4.4 ms ($n = 657$). There was a statistically significant difference in onset latency when the stimulus was applied in the presence or absence of background EMG ($P \leq 0.001$, Mann–Whitney). The mean latency when stimulation was applied in the presence of background muscle activity was 9.7 ± 3.3 ms ($n = 371$) compared with 12.1 ± 5.2 ms ($n = 286$) in the absence of background EMG activity. As noted above, higher stimulus intensities also produced shorter delays to EMG activation.

Variety of Responses to Stimulation

EMG responses to stimulation observed in this study fell into 3 categories—pE, pI, and tEI—as described earlier. However, subtle variations within these categories are noteworthy. Figure 5A illustrates an example of a consistent level of excitatory modulation for the duration of the stimulation, whereas Figure 5B illustrates an extreme example of an initial excitatory response yielding to either strong inhibitory interactions or a near complete inability to follow high-frequency modulation for the duration of stimulation. Although this record was obtained during extension when FDP was inactive, stimulation applied during flexion in the presence of background EMG confirmed a predominately excitatory effect. Figure 5C illustrates a dynamic strengthening and subsequent attenuation in EMG activity throughout the duration of the stimulation. These responses convey an interesting competition between excitatory and inhibitory networks within the brain and spinal cord. Often, this interplay leads the resulting EMG to transition from an excitatory response to an inhibitory response, possibly resulting from either greater latencies associated with the activation of inhibitory networks or stronger
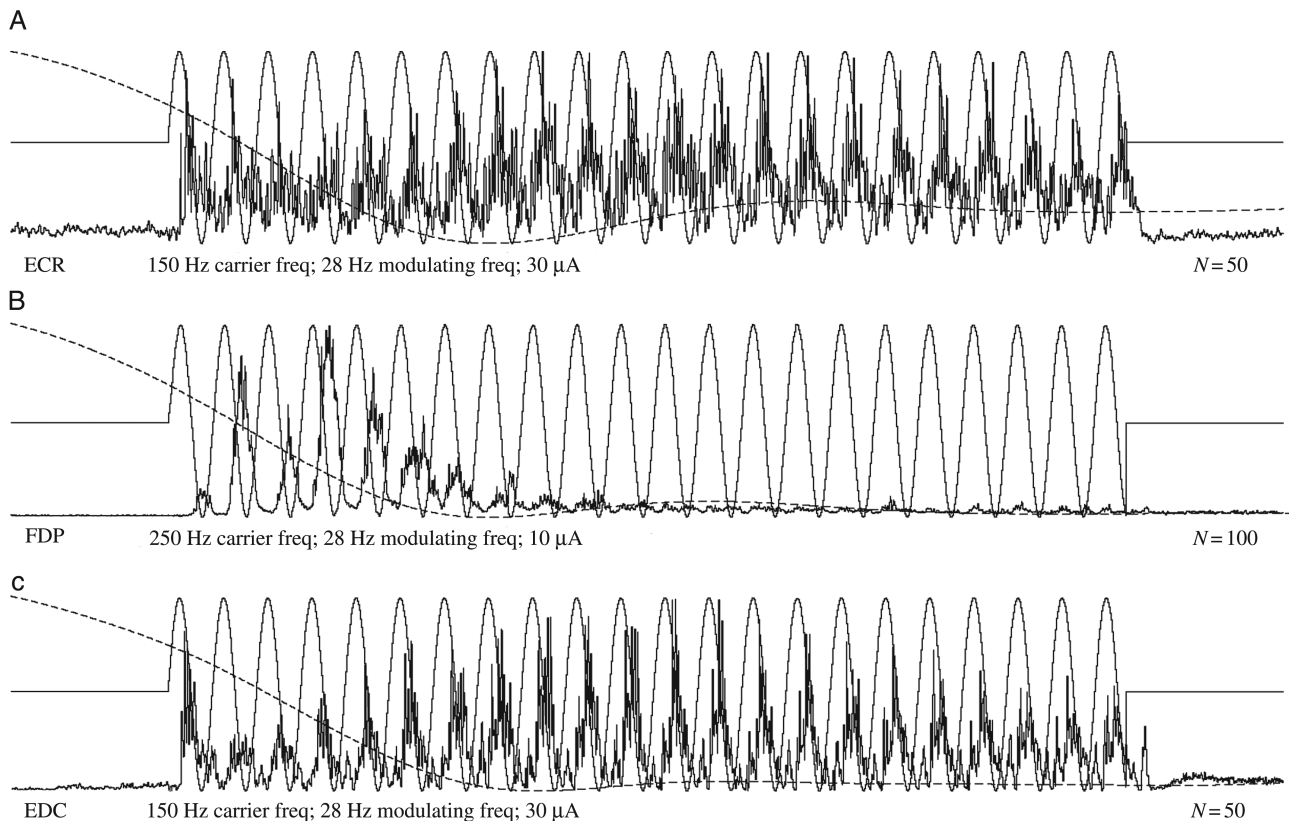
Figure 5. (A) Consistent modulation throughout stimulation. (B) Strong excitatory responses followed by almost complete loss of modulation after about 10 cycles. (C) Waxing and waning of EMG excitatory responses throughout the stimulus train. For muscle abbreviations, see Materials and Methods. Wrist position record (gray line) is superimposed on each EMG record, and ranges from 40° ± 10 in flexion to 30° ± 15 in extension. The stimulus modulation signal is shown as a sinusoidal line superimposed on the EMG records.

initial excitatory responses that eventually give way to building inhibitory tone.

Discussion

The timing of muscle activity resulting from modulations in descending cortical output remains an underlying question of interest in the study of neural encoding. Many previous studies have reported consistently greater latencies between cortical activity and the onset of muscle activity during natural movements than would be expected from the minimum conduction time through the same pathway. Conduction studies using StTA and SpTA have reported minimum conduction times through the forelimb cortico-muscle pathway of 6.7–9.8 ms, depending on the specific muscle tested (Cheney and Fetz 1980; Lemon et al. 1986; McKiernan et al. 1998; Park et al. 2004). In contrast, numerous studies have reported latencies of 60–122 ms from population cortical activity to movement or EMG onset during natural movement (Evarts 1972; Porter and Lewis 1975; Thach 1975; Cheney and Fetz 1980; Lamarre et al. 1981; Wannier et al. 1991; Porter and Lemon 1993).

There are several hypotheses regarding the nature of the observed discrepancy in timing. One hypothesis suggests that the disparity in timing may be due to plateau potentials in the dendritic currents of motoneurons, resulting from persistent inward currents (Morrow and Miller 2003; Shapiro and Lee 2007; Binder et al. 2011). These plateau potentials may act as a low-pass filter to both amplify and substantially delay the incoming signals.

Plateau potentials could produce a consistent delay in the expression of cortical activity at the muscle level. Moreover, this delay would be present throughout the entire movement, rather than solely at movement onset. Plateau potentials have been suggested as a possible explanation for the results obtained by Morrow and Miller (2003), in which they observed optimal fits between cortical activity and EMG activity using a time delay of 50 ms.

Another hypothesis is that activation of motoneurons may require integration of signals from both direct corticospinal pathways and indirect, multisynaptic pathways (Schieber and Rivlis 2007). These multisynaptic pathways could substantially increase the delay from cortical activity to EMG activity, although it would require a highly indirect route to account for the large discrepancy between the minimum conduction time and the cortical cell to muscle delay measured during active movement. Of course, it is well known that most corticospinal connections in the macaque monkey terminate in the intermediate lamina of the spinal cord rather than lamina IX containing motoneuron cell bodies. This interneuronal network might be part of the spinal pattern generator for rhythmic, stereotyped movements. The substantial delay resulting from integration of such pathways should be present not only at the onset of movement but also for the duration of the active movement.

Alternatively, the disparity may be due to the time required for the motoneurons to achieve firing threshold from a hyperpolarized inactive state. This requires summation of converging EPSPs from corticospinal and other inputs to motoneurons. The

time to reach firing threshold could pose a significant delay during the initiation of movement; however, the discrepancy in timing should be absent during active movement once the motoneurons are actively firing. If time to achieve threshold is a significant contributing factor to the delay between cortical cell activation and EMG activity, then the delay should approach the minimum conduction time through the pathway if the motoneurons are already active.

Results presented in this study are relevant to the timing issue in 2 respects. First, our results show that when the cortical output network and associated brainstem and spinal cord networks are activated with electrical stimulation in a sinusoidal pattern of modulation sufficient to produce overt driving of EMG activity, the EMG is phase-shifted relative to the stimulus signal by an amount approaching the minimum time required for conduction through the pathway from cortex to muscle. One might argue that this is a foregone conclusion because each individual stimulus will essentially produce a poststimulus facilitation effect. However, this is not the case. Individual stimuli at the intensities we have used do not generally produce any observable effect in the raw EMG record. Also, we tested many cortical site–muscle pairs (Table 2) that did not show any poststimulus effect, but did produce clear EMG modulation with high-frequency sinusoidal stimulation. The EMG modulation from stimulation at these sites had timing that was not significantly different from sites that did produce poststimulus facilitation in stimulus-triggered averages (see Results). Presumably, neurons activated at these sites lack the most direct linkages to motoneurons. This result shows that a modulated output signal from a population of motor cortex neurons, after being transmitted through the synaptic network to motoneurons, can produce corresponding modulation of EMG activity with a delay that is only a few milliseconds greater than the expected minimum conduction delay from cortex to muscle. This result argues against the plateau potential hypothesis and the multisynaptic pathway integration hypothesis and favors, although does not prove, the "need to reach threshold" hypothesis. Processes related to plateau potentials or multisynaptic pathway integration should have delayed signal transmission related to sinusoidal stimulation just as they would delay signal transmission of voluntary movement-related cortical signals. However, we cannot rule out that peculiarities in the nature of cortical activity generated by electrical stimulation might be evading these mechanisms. For instance, the rapid and synchronous activation of cells brought about with single-electrode stimulation could yield different results compared with the gradual and asynchronous activation associated with voluntary movement.

Also, supporting the "need to reach threshold" hypothesis is the fact that the phase shift from the onset of stimulation to the onset of EMG activity was greater when stimulation was applied in the absence of EMG activity compared with stimulation when background EMG activity was present. The fact that the difference was small compared with the delay between cortical activation and EMG/movement onset is likely due to a fundamental difference between the activation of cortical neurons using stimulation compared with natural activation during initiation of voluntary movement. Our stimulation method produces abrupt, synchronous and intense activation of cortical cells. As a consequence, at stimulus onset as well as throughout stimulation, a large number of cortical cells are rapidly and simultaneously activated yielding a large, relatively synchronous input volley to motoneurons bringing them to threshold quickly. In contrast, during initiation of natural voluntary movements, the onset of cortical cell firing is asynchronous with gradual recruitment of the requisite number of cells over a period of several

hundred milliseconds or more for a self-paced movement (Cheney and Fetz 1980). Of course, the well-established set-related activation of cortical neurons in preparation for a movement would tend to increase excitability, not only of cortical neurons, but also of motoneurons, and reduce the time to reach motoneuron firing threshold and, hence, movement reaction time (Tanji and Evarts 1976).

Our conclusions are supported by the results of Griffin et al. (2008) who measured the time difference between peaks in CM cell firing rate relative to corresponding peaks in target muscle EMG activity during a reach-to-grasp arm movement task. In this task, the peaks in activity occurred on a background of EMG activity and more closely matched the conditions of our sinusoidal stimulation. The average peak in CM cell activity led the peak in EMG activity by 23 ms. Although this is still greater than the phase difference observed in our study (12.8 ms at 10 µA), it is, nevertheless, in much closer agreement to our sinusoidal stimulation than to delays of 60–122 ms obtained from measurements of cortical cell onset to EMG/movement onset starting from rest or an inhibited condition. Another example of a condition in which natural activation of CM cells occurred in the presence of background EMG activity involves applying torque pulses at the wrist, which stretched the cell's target muscles (Cheney and Fetz 1985). Rapid stretch of the target muscles brought about brisk and potent activation of CM cells, making it a good comparison with the rapid activation of cortical cells with stimulation in the current study. Torque pulse evoked muscle stretch also elicited rapid reflex responses in muscle including an M1 response, believed to be spinal in origin, and an M2 response, believed to be cortical in origin. The mean onset latency of CM cell responses to torque pulse perturbations of movement was 23.4 ms compared with 27.9 ms for M2 onset, leaving a difference of 4.5 ms for conduction time from cortex to muscle. Actual conduction time was estimated to be 7.0 ms based on the mean phase shift of postspike facilitation. Of course, in this case, as with the timing study of Griffin et al. (2008) for natural movement-related activity, motoneurons will be receiving additional sources of input beyond corticospinal-related inputs. Nevertheless, it is noteworthy that, in this case, with abrupt and potent activation of cortical cells, the time delay between the onset of cortical cell activity and muscle activity is consistent with the conduction time from cortex to muscle, in agreement with the results presented in this paper.

Summary and Conclusions

Although the time delay between peaks in the frequency-modulated cortical stimulus train and corresponding EMG modulation varied somewhat with the stimulus parameters, the overall mean phase shift of excitatory modulation across all parameters determined via cross-correlation analysis (11.5 ± 5.6 ms) matched closely the conduction time through the cortex-to-muscle pathway derived from stimulus-triggered averaging of EMG activity as the peak PStF latency (12.6 ± 2.0 ms) computed at the same sites. These results demonstrate that, during active movement, cortical output can modulate muscle activity at latencies approaching the minimum conduction time through the cortico-muscle pathway. Moreover, the delay between the onset of stimulation and the corresponding onset of EMG activity increased when stimulation was applied in the absence of background EMG activity compared with active EMG. The results support the hypothesis that the longer time delays reported for the timing between natural cortical cell activation and muscle activation during voluntary movement are due largely to the time required to bring motoneurons to firing threshold from a hyperpolarized state.

Funding

Notes

References

Baker SN, Lemon RN. 1998. Computer simulation of post-spike facilitation in spike-triggered averages of rectified EMG. J Neurophysiol. 80:1391–1406.

Begovic H, Zhou GQ, Li T, Wang Y, Zheng YP. 2014. Detection of the electromechanical delay and its components during voluntary isometric contraction of the quadriceps femoris muscle. Front Physiol. 5:494.

Binder MD, Heckman CJ, Powers RK. 2011. The physiological control of motoneuron activity. In: Rowell LB, Shepherd JT, editors. Handbook of Physiology. New York, NY: Oxford University Press. p. 3–53.

Buys EJ, Lemon RN, Mantel GW, Muir RB. 1986. Selective facilitation of different hand muscles by single corticospinal neurones in the conscious monkey. J Physiol. 381:529–549.

Cheney PD, Fetz EE. 1980. Functional classes of primate corticomotoneuronal cells and their relation to active force. J Neurophysiol. 44:773–791.

Cheney PD, Fetz EE. 1985. Comparable patterns of muscle facilitation evoked by individual corticomotoneuronal (CM) cells and by single intracortical microstimuli in primates: evidence for functional groups of CM cells. J Neurophysiol. 53:786–804.

Evarts EV. 1972. Contrasts between activity of precentral and postcentral neurons of cerebral cortex during movement in the monkey. Brain Res. 40:25–31.

Griffin DM, Hudson HM, Belhaj-Saif A, McKiernan BJ, Cheney PD. 2008. Do corticomotoneuronal cells predict target muscle EMG activity? J Neurophysiol. 99:1169–1986.

Griffin DM, Hudson HM, Belhaj-Saif A, Cheney PD. 2014. EMG activation patterns associated with high frequency, long duration intracortical microstimulation of primary motor cortex. J Neurosci. 34:1647–1656.

Houk JC, Dessem DA, Miller LE, Sybirska EH. 1987. Correlation and spectral analysis of relations between single unit discharge and muscle activities. J Neurosci Methods. 21:201–224.

Humphrey DR, Corrie WS. 1978. Properties of pyramidal tract neuron system within a functionally defined subregion of primate motor cortex. J Neurophysiol. 41:216–243.

Jankowska E, Padel Y, Tanaka R. 1975. The mode of activation of pyramidal tract cells by intracortical stimuli. J Physiol. 249:617–636.

Lamarre Y, Spidalieri G, Lund JP. 1981. Patterns of muscular and motor cortical activity during a simple arm movement in the monkey. Can J Physiol Pharmacol. 59:748–756.

Lemon RN, Mantel GW, Muir RB. 1986. Corticospinal facilitation of hand muscles during voluntary movement in the conscious monkey. J Physiol. 381:497–527.

McKiernan BJ, Marcario JK, Karrer JH, Cheney PD. 1998. Corticomotoneuronal postspike effects in shoulder, elbow, wrist, digit, and intrinsic hand muscles during a reach and prehension task. J Neurophysiol. 80:1961–1980.

McKiernan BJ, Marcario JK, Karrer JH, Cheney PD. 2000. Correlations between corticomotoneuronal (CM) cell postspike effects and cell-target muscle covariation. J Neurophysiol. 83:99–115.

Mewes K, Cheney PD. 1991. Facilitation and suppression of wrist and digit muscles from single rubromotoneuronal cells in the awake monkey. J Neurophysiol. 66:1965–1977.

Miller LE, van Kan PL, Sinkjaer T, Andersen T, Harris GD, Houk JC. 1993. Correlation of primate red nucleus discharge with muscle activity during free-form arm movements. J Physiol. 469:213–243.

Morrow MM, Miller LE. 2003. Prediction of muscle activity by populations of sequentially recorded primary motor cortex neurons. J Neurophysiol. 89:2279–2288.

Park MC, Belhaj-Saif A, Cheney PD. 2000. Chronic recording of EMG activity from large numbers of forelimb muscles in awake macaque monkeys. J Neurosci Methods. 96:153–160.

Park MC, Belhaj-Saif A, Cheney PD. 2004. Properties of primary motor cortex output to forelimb muscles in rhesus macaques. J Neurophysiol. 92:2968–2984.

Porter R, Lemon RN. 1993. Corticospinal function and voluntary movement. Oxford: Clarendon.

Porter R, Lewis MM. 1975. Relationship of neuronal discharges in the precentral gyrus of monkeys to the performance of arm movements. Brain Res. 98:21–36.

Rathelot JA, Strick PL. 2006. Muscle representation in the macaque motor cortex: an anatomical perspective. Proc Natl Acad Sci USA. 103:8257–8262.

Rathelot JA, Strick PL. 2009. Subdivisions of primary motor cortex based on cortico-motoneuronal cells. Proc Natl Acad Sci USA. 106:918–923.

Schieber MH, Rivlis G. 2007. Partial reconstruction of muscle activity from a pruned network of diverse motor cortex neurons. J Neurophysiol. 97:70–82.

Shapiro NP, Lee RH. 2007. Synaptic amplification versus bistability in motoneuron dendritic processing: a top-down modeling approach. J Neurophysiol. 97:3948–3960.

Tanji J, Evarts EV. 1976. Anticipatory activity of motor cortex neurons in relation to direction of an intended movement. J Neurophysiol. 39:1062–1068.

Tehovnik EJ. 1996. Electrical stimulation of neural tissue to evoke behavioral responses. J Neurosci Methods. 65:1–17.

Thach WT. 1975. Timing of activity in cerebellar dentate nucleus and cerebral motor cortex during prompt volitional movement. Brain Res. 88:233–241.

Townsend BR, Paninski L, Lemon RN. 2006. Linear encoding of muscle activity in primary motor cortex and cerebellum. J Neurophysiol. 96:2578–2592.

Wannier TM, Maier MA, Hepp-Reymond MC. 1991. Contrasting properties of monkey somatosensory and motor cortex neurons activated during the control of force in precision grip. J Neurophysiol. 65:572–589.